Neuron, Vol. 40, 551–561, October 30, 2003, Copyright ©2003 by Cell Press

A Diacylglycerol-Gated Cation Channel in Vomeronasal Neuron Dendrites Is Impaired in *TRPC2* Mutant Mice: Mechanism of Pheromone Transduction

Philippe Lucas,[1] Kyrill Ukhanov, Trese Leinders-Zufall,* and Frank Zufall*
Department of Anatomy and Neurobiology and Program in Neuroscience
University of Maryland School of Medicine
Baltimore, Maryland 21201

Summary

Vomeronasal sensory neurons play a crucial role in detecting pheromones, but the chemoelectrical transduction mechanism remains unclear and controversial. A major barrier to the resolution of this question has been the lack of an activation mechanism of a key transduction component, the TRPC2 channel. We have identified a Ca^{2+}-permeable cation channel in vomeronasal neuron dendrites that is gated by the lipid messenger diacylglycerol (DAG), independently of Ca^{2+} or protein kinase C. We demonstrate that ablation of the *TRPC2* gene causes a severe deficit in the DAG-gated channel, indicating that *TRPC2* encodes a principal subunit of this channel and that the primary electrical response to pheromones depends on DAG but not $Ins(1,4,5)P_3$, Ca^{2+} stores, or arachidonic acid. Thus, a previously unanticipated mechanism involving direct channel opening by DAG underlies the transduction of sensory cues in the accessory olfactory system.

Introduction

The vomeronasal organ (VNO) of mammals, a part of the accessory olfactory system, plays an essential role in the detection of pheromones, molecular cues emitted by individuals of the same species that elicit various neuroendocrine changes and mediate stereotyped behavioral repertoires. The VNO has emerged as an excellent system to address one of the major challenges in neuroscience: to decipher the precise signaling codes that initiate complex social behaviors (Keverne, 2002). Recent studies have begun to explore this question by using gene targeting of specific signaling molecules that are expressed either by all vomeronasal sensory neurons (VSNs) (Leypold et al., 2002; Stowers et al., 2002) or by distinct subsets of VSNs (Del Punta et al., 2002; Loconto et al., 2003; Norlin et al., 2003). These studies clearly implicate populations of VSNs as playing an integral part in directly initiating pheromone-mediated behaviors, including aggressive interactions, territorial and dominance recognition, and mate choice (for a review, see Dulac and Torello, 2003). Recordings from single neurons in the accessory olfactory bulb of mice engaged in natural behaviors have supported this concept (Luo et al., 2003). It is important to note, however, that the VNO recognizes also a variety of nonpheromonal cues (Johnston, 1998; Sam et al., 2001; Trinh and Storm, 2003).

How are molecular cues transduced into neural signals in the VNO? VSNs respond to sensory stimulation with a receptor-mediated excitatory response leading to increased action potential firing and elevated intracellular Ca^{2+} (Trotier et al., 1998; Inamura et al., 1999; Leinders-Zufall et al., 2000; Holy et al., 2000; Inamura and Kashiwayanagi, 2000; Cinelli et al., 2002; Del Punta et al., 2002; Boschat et al., 2002; Spehr et al., 2002), but the molecular mechanism underlying this response remains unclear and controversial. Some of this controversy arises because it has not been possible to identify the specific mechanism that activates one of the key components of the signaling cascade of VSNs, the transient receptor potential channel TRPC2 (also known as TRP2). The *TRPC2* gene, an important marker for the evolution of vomeronasal signaling in primates (Liman and Innan, 2003; Zhang and Webb, 2003), encodes a protein that is expressed in all VSNs and specifically localized to the sensory microvilli of these cells (Liman et al., 1999; Menco et al., 2001). Genetic ablation of *TRPC2* markedly impairs the sensory response to pheromones (Leypold et al., 2002; Stowers et al., 2002). Given that most members of the mammalian TRPC subfamily (Montell et al., 2002) appear to be regulated by the activity of phospholipase C (PLC), the enzyme that hydrolyzes phosphatidylinositol-4,5-bisphosphate (PIP_2) into inositol 1,4,5-trisphosphate [$Ins(1,4,5)P_3$] and diacylglycerol (DAG), it has been suggested that TRPC2 depends also on a PLC-mediated signaling cascade (Liman et al., 1999; Dulac and Torello, 2003). Two lines of evidence support this view. First, in several species, biochemical studies have reported increased $Ins(1,4,5)P_3$ levels in response to sensory stimulation in the VNO (Luo et al., 1994; Kroner et al., 1996; Wekesa and Anholt, 1997; Krieger et al., 1999; Sasaki et al., 1999; Cinelli et al., 2002). Second, pheromone-induced action potential and Ca^{2+} responses in VSNs are blocked by a pharmacological antagonist of PLC (Inamura et al., 1997a; Holy et al., 2000; Spehr et al., 2002).

Despite these extensive investigations, it is still a mystery whether TRPC2 forms a functional ion channel in VSNs, and if so, how PLC signaling leads to channel opening. Heterologous expression studies proved unsatisfactory with regard to this question (Vannier et al., 1999; Hofmann et al., 2000, 2002) and efforts directed toward measuring native channels in intact VSNs have failed thus far. In the absence of concrete information on an activation mechanism for TRPC2, four distinct transduction models have been put forward. First, TRPC2 functions as a store-depletion-activated capacitative Ca^{2+} entry channel (known as CRAC channel), possibly through direct interaction between an $Ins(1,4,5)P_3$ receptor and TRPC2 (Vannier et al., 1999; Brann et al., 2002). In this model, channel activation is triggered by Ca^{2+} store depletion. Second, the transduction channels are directly gated by $Ins(1,4,5)P_3$ (summarized by Cinelli

*Correspondence: fzufa001@umaryland.edu (F.Z.), tlein001@umaryland.edu (T.L.-Z.)
[1] Present address: INRA, Unité de Phytopharmacie et des Médiateurs Chimiques, 78026 Versailles Cedex, France.

et al., 2002). This model is based mainly on reports of a membrane current following dialysis of Ins(1,4,5)P_3 into VSNs (Taniguchi et al., 1995; Inamura et al., 1997b; Taniguchi et al., 2000). Third, a newly identified Ca^{2+}-activated nonselective cation (CaNS) channel may either directly mediate VSN transduction or amplify the primary sensory response (Liman, 2003). Fourth, the transduction channels are directly activated by arachidonic acid, a polyunsaturated fatty acid (PUFA) that, in living cells, is synthesized from DAG by a DAG lipase or from phospholipids by phospholipase A_2 (Spehr et al., 2002).

To resolve this matter and to define the nature of the signal transduction mechanism in the VNO, we set out to identify and characterize the native ion channels that are encoded by *TRPC2*. We now report the identification of a novel DAG-gated cation channel in wild-type mouse VSNs and that ablation of the *TRPC2* gene causes a severe deficit in this channel. We characterize the conductance induced by natural pheromones in intact, voltage-clamped VSNs and provide evidence that it is mediated by DAG but not Ins(1,4,5)P_3 or Ca^{2+} store depletion. Finally, we show that blockade of enzymes that synthesize arachidonic acid and other PUFAs does not inhibit the pheromone-evoked conductance.

Results and Discussion

A DAG-Gated Ion Channel in VSN Dendrites

The experimental design we employed to identify native ion channels mediating VSN transduction was based on four assumptions. First, the ion channels are likely to be found at the dendritic tip of VSNs. Second, they are likely to be regulated, directly or indirectly, by products of PLC activity. Third, they are likely to be defective in *TRPC2*$^{-/-}$ VSNs. Fourth, they are expected to exhibit functional properties consistent with those of the pheromone-induced conductance.

To search for channels that meet these four criteria, we performed patch-clamp recordings from excised inside-out patches of plasma membrane taken from the dendritic tips of freshly dissociated mouse VSNs (Figure 1A). We cannot yet determine whether these patches are from the microvilli or dendritic knob or both. Characteristic channel activity recorded from these patches is shown in Figure 1B (holding potential, −80 mV; see also Figure 2). Control recordings obtained in symmetrical divalent cation-free solutions with Na^+ as the sole cation showed no or very infrequent brief channel openings. To test whether a conductance exists in these patches that is controlled by products of PLC activity, we first explored a potential role of DAG, one of the two second messengers generated by PLC. Addition of the endogenous DAG analog 1-stearoyl-2-arachidonoyl-*sn*-glycerol (SAG, 100 μM) to the bathing medium (i.e., the cytosolic membrane face of the patch) produced an unanticipated increase in channel activity giving rise to a sustained inward current (Figure 1B). This effect was accompanied by an increased noise level that reflects fluctuations in the activity of single channels. The presence of ATP, GTP, Ca^{2+}, or Mg^{2+} in the bath was not required for activation of this current. The current could not be activated by Ca^{2+} alone (without added SAG), indicating that the underlying channels must be different from the Ca^{2+}-activated channels reported by Liman (2003). A total of 38 patches were analyzed, of which 33 (87%) showed a response to SAG or other DAG analogs. Most patches possessed multiple channels (up to 35); a few had only a single channel (see below).

The current-voltage (I-V) relationship of the SAG-activated conductance was nearly linear, with a reversal potential of 1.7 ± 2.4 mV (Figure 1C, n = 6). An outward current was also measurable when Cs^+ or Ca^{2+} was the only intracellular cation (Figures 1D and 1E). SAG-induced outward currents were abolished when all intracellular cations were replaced with *N*-methyl-D-glucamine ($NMDG^+$) (Figure 1F). We investigated relative ionic permeability by determining reversal potentials under bi-ionic conditions (Lewis, 1979) with Na^+ as the sole cation in the pipette solution. The relative permeabilities P_{Ca}/P_{Na} and P_{Cs}/P_{Na} were 2.7 ± 0.7 (n = 3) and 1.5 ± 0.3 (n = 5), respectively. Thus, SAG activates a nonselective cation conductance that is permeable for Na^+, Cs^+, and Ca^{2+} but not for $NMDG^+$.

DAG Activates a 42-pS Cation Channel

Single-channel activity was analyzed in five patches that contained only one or very few channels. Following the addition of SAG (10 μM), we observed single-channel currents with a mean unitary current amplitude of −3.3 ± 0.5 pA at a holding potential of −80 mV (Figures 2A and 2B). Amplitude histograms were well fitted by a single Gaussian curve (Figures 2C and 2D). A small shoulder in the lower amplitude region of the distribution of openings suggests one or more subconductance states (Figure 2D). Like the macroscopic currents, SAG-induced single-channel currents exhibited a nearly linear I-V relationship with a slope conductance of 42 pS in symmetrical 150 mM Na^+ solution (Figure 2E). Replacement of Na^+ by $NMDG^+$ in the intracellular solution resulted in a shift of the reversal potential to 80 mV and abolished the outward current (data not shown). Together, the results of Figures 1 and 2 demonstrate that a novel Ca^{2+}-permeable cation channel that can be activated by DAG in a membrane-delimited fashion exists in distal dendrites of mouse VSNs. Importantly, this channel shows none of the hallmarks of store depletion-activated capacitative Ca^{2+} entry channels (Parekh and Penner, 1997; Lewis, 1999), such as high Ca^{2+} selectivity, low unitary conductance, or inward rectification.

Ligand Specificity

Next, we investigated the ligand specificity of this channel by comparing the effectiveness of SAG with two other DAG analogs: 1-oleoyl-2-acetyl-*sn*-glycerol (OAG) and 1,2-dioctanoyl-*sn*-glycerol (DOG, 100 μM each). Each of these analogs produced a robust increase in channel activity in inside-out patches (Figures 3A and 3B), with DOG being somewhat less effective than SAG or OAG (SAG: I_{mean} = −36 ± 52 pA, n = 16; OAG: I_{mean} = −43 ± 7 pA, n = 4; DOG: I_{mean} = −17 ± 13 pA, n = 12). The monoacylglycerol 1-oleoyl-glycerol (OG, 100 μM) did not evoke channel openings, demonstrating the specificity of channel activation (Figure 3C, n = 3). We also examined the effect of the second product of PLC activity, Ins(1,4,5)P_3. However, in no case did we

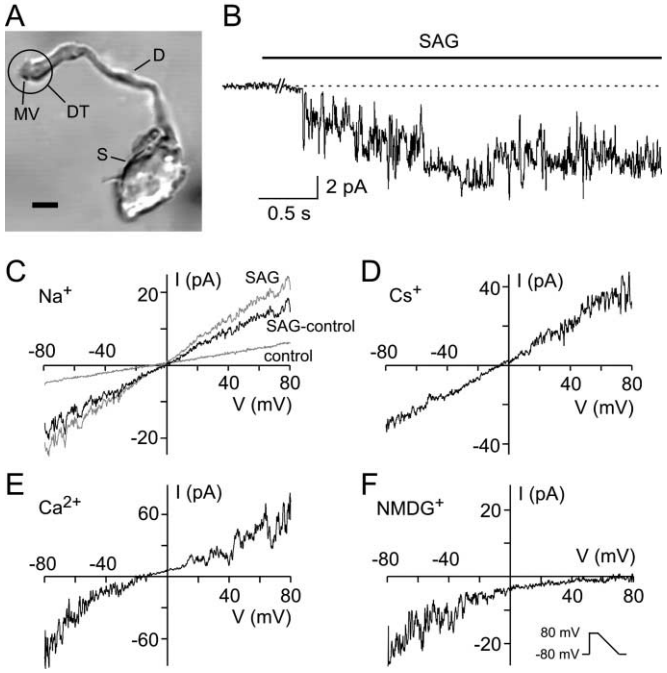

Figure 1. A DAG-Activated Cation Channel in Inside-Out Patches from the Dendritic Tip of VSNs

(A) Micrograph showing an isolated mouse VSN. MV, microvilli; D, dendrite; S, soma. Plasma membrane patches were taken from the encircled area denoted as dendritic tip (DT). Scale bar, 3 μm.

(B) Sustained channel activity evoked by the addition of SAG (100 μM) to the bath. Holding potential, −80 mV. Bandwidth, 0–2 kHz.

(C–F) I-V relationship of SAG-induced conductance obtained when Na^+ (C), Cs^+ (D), Ca^{2+} (E), or $NMDG^+$ (F) was the sole intracellular cation. Extracellular pipette solution contained Na^+ as the sole cation. Curves were obtained in response to voltage ramps (duration, 100 ms; slope −1.6 mV/ms) as indicated in (F). Leak conductance (control, gray) measured immediately before stimulus application was subtracted digitally.

observe noticeable channel activity in response to Ins(1,4,5)P_3 (50 or 100 μM; Figure 3D; n = 11).

The DAG-Gated Channel Is Defective in *TRPC2*$^{-/-}$ VSNs

Is the TRPC2 subunit required for normal function of the DAG-gated channel? If so, the DAG-activated channel should exhibit specific defects in VSNs from mice that harbor a targeted deletion in the *TRPC2* gene. To test this prediction, we investigated DAG-induced currents by using whole-cell patch-clamp recordings in voltage-clamped VSNs isolated from wild-type (wt) or *TRPC2*$^{-/-}$ mice. In Figures 4A–4C, the membrane potential of a wt VSN was stepped from 0 to ±80 mV (in 10 mV increments) under three different conditions: (1) in extracellular control solution; (2) in control solution containing 50 μM SAG; and (3) in the presence of 50 μM SAG in an extracellular solution in which $NMDG^+$ was the sole cation. Wild-type VSNs exhibited a prominent SAG-activated conductance which occurred without added ATP, GTP, Ca^{2+}, or Mg^{2+} to the pipette solution (Figure 4B). This SAG-induced conductance was observed in every VSN that exhibited a morphologically intact dendrite containing microvilli (33 of 33); however, VSNs that had lost their dendrite during the isolation procedure did not show this response (n = 4), indicating that the DAG-

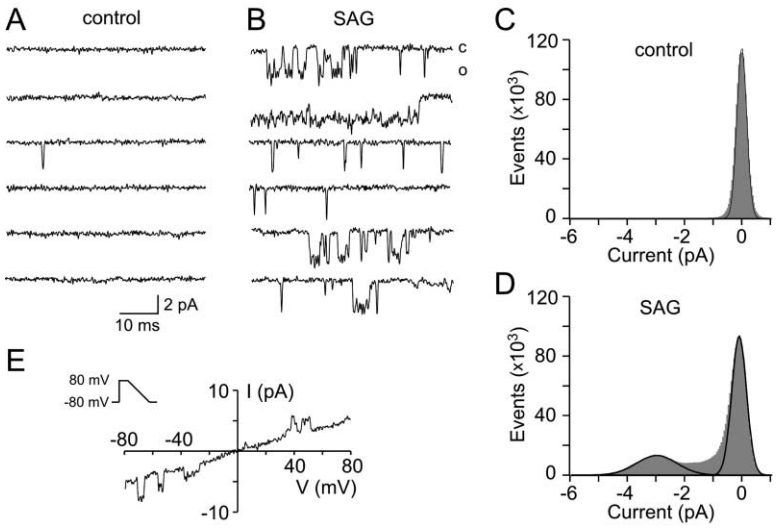

Figure 2. DAG Activates a 42-pS Channel that Shows None of the Hallmarks of Capacitative Ca^{2+} Entry Channels

(A) Control recordings before SAG application showed no activity or only an occasional brief channel opening.

(B) Examples of single-channel events evoked by the continuous application of SAG (10 μM). Holding potential, −80 mV. On average, these events lasted for a few milliseconds. We also observed bursts of openings that lasted for tens or even hundreds of milliseconds.

(C and D) Amplitude histograms of single-channel events before (C) and after the application of 10 μM SAG (D). In both cases, a continuous stretch of activity lasting for 200 s was analyzed. The data were fitted by Gaussian curves using the maximum likelihood method. The peak of the distribution of openings was at −3.04 pA (D). Bandwidth, 0–2 kHz.

(E) I-V relationship of SAG-activated single-channel current in response to a voltage ramp as indicated in the figure.

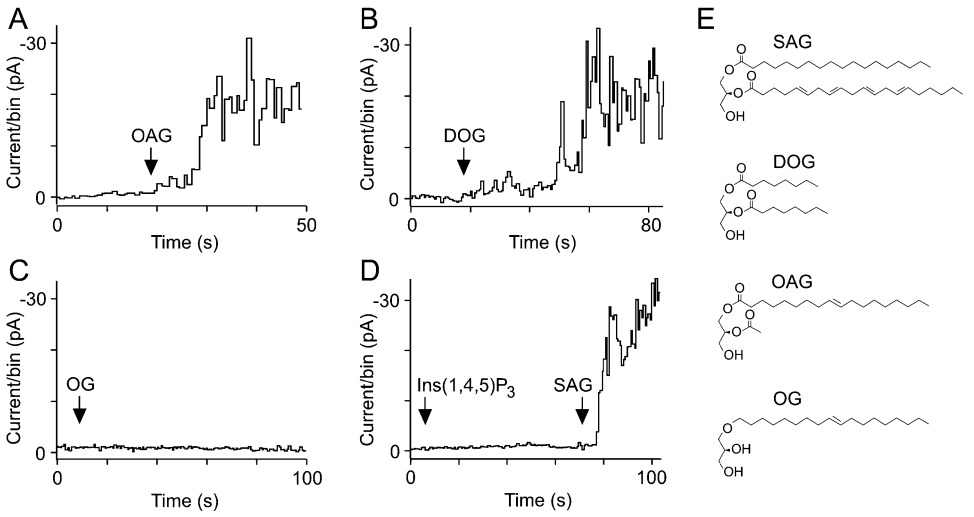

Figure 3. Ligand Specificity of the DAG-Activated Channel in Excised Patches

(A–D) Channel activity in response to the application of OAG (100 μM) (A), DOG (100 μM) (B), OG (100 μM) (C), Ins(1,4,5)P_3 (100 μM) (D), and SAG (100 μM) (D). Stimulants were added to the bath at the times indicated by the arrows. Each recording was from a different inside-out membrane patch. Holding potential, −80 mV. Channel activity is plotted as mean current per 500 ms bin. Note that OG and Ins(1,4,5)P_3 were ineffective in inducing channel activation.

(E) Chemical structures of the lipids used to characterize the DAG-gated channel.

gated channels are enriched in the VSN dendrite and microvilli. Consistent with the properties of single-channel currents, the whole-cell conductance exhibited a nearly linear I-V relationship, with a reversal potential close to 0 mV (Figure 4G). We observed a leftward shift in this potential, together with an elimination of the inward current, after replacement of all extracellular cations by $NMDG^+$ (Figure 4G). A 15 min preincubation with one of two protein kinase C (PKC) inhibitors, staurosporine or calphostin C (1 μM each), did not inhibit activation of the conductance, indicating a PKC-independent activation mechanism (n = 4). We also tested whether the effect of SAG was dependent upon PLC; PLC not only serves to produce DAG but it can also be activated by this lipid (Goñi and Alonso, 1999; Estacion et al., 2001). However, an antagonist of PLC, U-73122 (10 μM), did not attenuate the SAG-evoked conductance (n = 4, see Figure 7B), ruling out that the effect of SAG on the channel reported here was through stimulation of PLC.

In contrast, VSNs from *TRPC2*$^{-/-}$ mice displayed a striking deficit in the SAG-induced response: SAG application failed to activate a large conductance in *TRPC2*$^{-/-}$ VSNs (Figures 4D, 4E, and 4F; n = 29). However, a drastically diminished residual response to SAG still existed in these cells (Figures 4E and 4F), consistent with the residual responses to pheromones observed in *TRPC2*$^{-/-}$ mice (Leypold et al., 2002). Comparison of the dose-dependence of averaged SAG-induced currents (at −70 mV) from multiple wt and *TRPC2*$^{-/-}$ VSNs shows that activation of the current is significantly reduced at all concentrations of SAG (between 10 μM and 100 μM) in VSNs lacking TRPC2 (Figure 4I). This deficit is most obvious at a concentration of 100 μM SAG, with a reduction in the maximum current to ≈8% of wt control (Figure 4I). Hence, genetic ablation of TRPC2 eliminates most of the SAG-induced current in single VSNs.

The residual SAG-activated conductance in *TRPC2*$^{-/-}$ VSNs displayed a similar reversal potential as the wt conductance (wt: $E_{rev} = -3.1 \pm 6.1$ mV, n = 33; *TRPC2*$^{-/-}$: $E_{rev} = -6.4 \pm 8.6$ mV, n = 21). However, it could be distinguished from the wt conductance by its characteristic shape of the I-V curve, showing marked inward rectification (Figure 4H, inset). This finding rules out that the reduction in overall amplitude of the SAG-activated conductance is simply the result of a downregulation of the number of DAG-gated channels in each *TRPC2*$^{-/-}$ VSN. Instead, it provides evidence that TRPC2 functions as a principal subunit of the DAG-gated channel. Conclusive proof of this notion will require functional gene transfer. The presence of a residual conductance in *TRPC2*$^{-/-}$ VSNs suggests that other channel subunits activated by DAG may exist in VSNs, although with strongly reduced efficacy. It remains to be seen whether these predicted channel subunits associate with TRPC2 to form a heteromultimeric channel complex or whether they form independent channels.

Pheromone- and DAG-Evoked Currents Share the Same Properties

Because TRPC2 plays a central role in the pheromone-evoked field potential recorded from VSN microvilli (Leypold et al., 2002), the DAG-gated channel must also play a central role in this pheromone response. The channel could serve as the primary conductance in a pheromone-stimulated second messenger cascade, or it could mediate a secondary amplification of the primary response. To distinguish between these possibilities, we directly compared the properties of pheromone- and SAG-evoked currents. For the analysis of pheromone-induced currents, we used a VNO slice preparation and obtained whole-cell patch-clamp recordings from optically identified VSNs (Leinders-Zufall et al., 2000). Under current clamp, local stimulation of the dendritic tip and microvilli with dilute urine (DU, 1/100), a rich source of

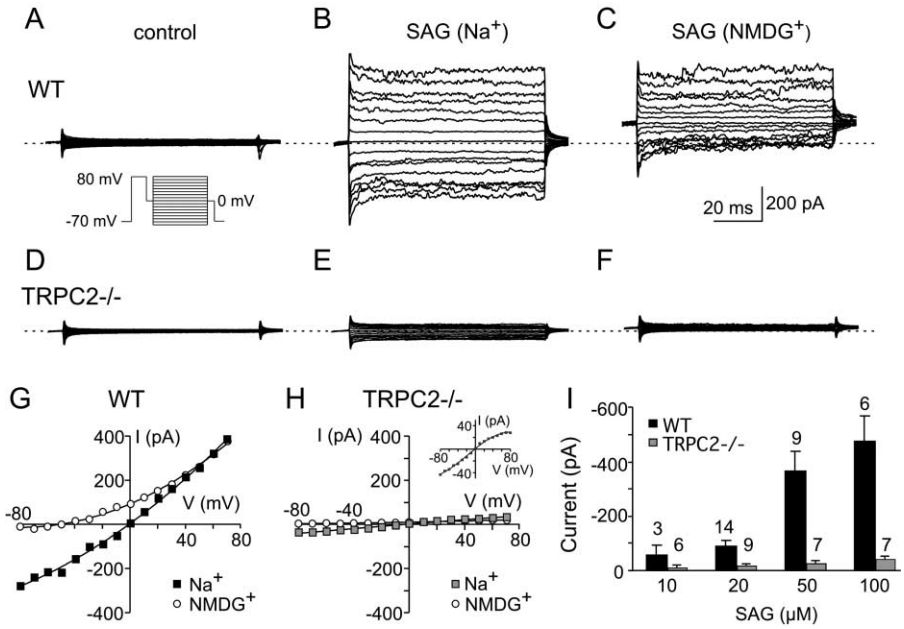

Figure 4. *TRPC2*$^{-/-}$ VSNs Display a Striking Defect in the Activation of the DAG-Gated Channel

(A–F) Representative families of whole-cell currents to a series of depolarizing and hyperpolarizing voltage steps (as indicated in the figure) recorded from an isolated wt (A, B, and C) or *TRPC2*$^{-/-}$ VSN (D, E, and F). VSNs were exposed successively to extracellular control solution (A and D), control solution containing 50 μM SAG (B and E), or 50 μM SAG in extracellular solution in which $NMDG^+$ was the sole cation (C and D). Experiments were performed in the presence of 1 μM tetrodotoxin to block voltage-gated Na^+ channels; voltage-activated K^+ channels were blocked by using a Cs^+-based pipette solution. Dotted line, zero current level.

(G and H) Plots of the steady-state I-V relationships of the SAG-induced responses shown above; (G), wt; (H), *TRPC2*$^{-/-}$. Solid rectangles, SAG-induced currents in control solution; open circles, SAG-induced currents in $NMDG^+$-based solution. Currents obtained before SAG application (control) were digitally subtracted from the curves. Data points were fit by a polynomial function. The inset in (H) shows a magnification of the curve obtained with Na^+. Note that the shape of this curve differed significantly from that in wt VSNs shown in (G).

(I) Comparison of the dose dependence of averaged SAG-induced currents (at −70 mV) from multiple wt (black bars) and *TRPC2*$^{-/-}$ VSNs (gray bars). Data are the means ± SEM for the number of cells indicated above each bar.

natural pheromones, produced a depolarizing receptor potential that generated robust action potential firing in a subset of VSNs (12 of 33, 36%) (Figure 5A). The size of the receptor potential varied considerably across responsive neurons, in accord with previous extracellular recordings of action potential activity (Inamura et al., 1999; Holy et al., 2000). Underlying the receptor potential is an ionic current that is the earliest electrical event in the transduction process. We measured this sensory current in voltage-clamped VSNs (n = 48) and found that urine- and SAG-evoked currents share the same properties (Figure 5).

First, in both cases the currents were inward; outward currents to urine were never observed at a normal holding potential of −70 mV (Figures 5B, 5D, and 5G). The size of the urine-evoked current ranged from −5 to −50 pA, similar to that evoked by low micromolar concentrations of SAG (Figure 4I).

Second, the I-V relationships for both the SAG-induced current (Figure 4G) and the urine-evoked current (Figure 5C) were virtually identical; they were both nearly linear and showed a reversal close to 0 mV (SAG: $V_{rev} = -3.1 \pm 6.1$ mV, n = 32; DU: $V_{rev} = -4.0 \pm 6.5$ mV, n = 9).

Third, changing the ionic composition in the bath altered both currents in an identical manner; like the SAG-induced current, the urine-evoked current was abolished at −70 mV after replacement of all extracellular cations by $NMDG^+$ (Figure 5D, n = 3). Furthermore, lowering the extracellular Ca^{2+} concentration from 1 mM to 10 μM increased the peak amplitude of both currents (Figure 5E; SAG: by 2.7-fold, n = 5; DU: by 2.5-fold, n = 6), suggesting that extracellular Ca^{2+} entering the transduction channel blocks the channel pore or serves as a negative feedback signal in channel activation or both.

Fourth, both currents showed the same pharmacological properties; 2-aminoethoxydiphenyl borate (2-APB, 50 μM), a compound that is known to block some TRP channels (Clapham et al., 2001) as well as store-operated Ca^{2+} entry (Bootman et al., 2002), eliminated the currents elicited by SAG (50 μM) and urine (Figures 5F and 5G; n = 12).

On the basis of these findings, we conclude that the DAG-gated channel reported here is the primary conductance pathway in the chemoelectrical transduction machinery of mouse VSNs.

Activation of the Pheromone Conductance Does Not Depend on Arachidonic Acid, PUFAs, Ins(1,4,5)P_3, or Store Depletion

TRP channels responsible for *Drosophila* phototransduction are activated by a variety of lipid messengers, including arachidonic acid and its downstream metabo-

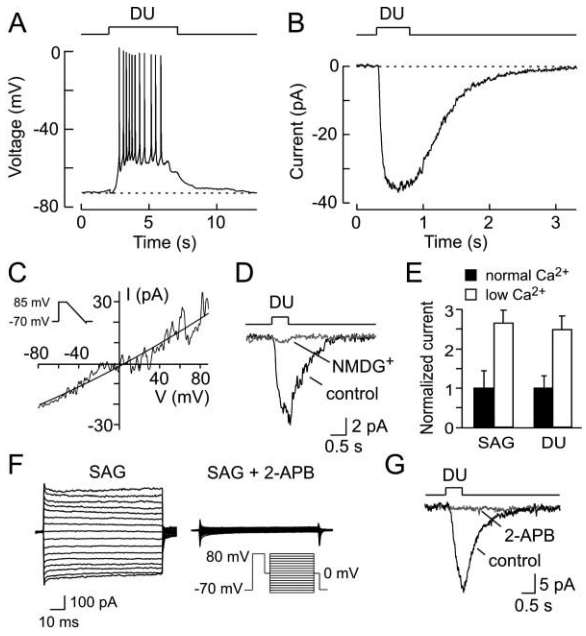

Figure 5. Pheromone- and DAG-Evoked Currents Share the Same Properties

(A) Focal stimulation of a current-clamped VSN with dilute urine (DU, 1/100) produces a depolarizing receptor potential leading to robust action potential discharges. K^+-based pipette solution.

(B) Under voltage clamp, sensory stimulation generates a rapidly activating and then deactivating inward current (the sensory current) with the following kinetic parameters: latency (measured as the time between triggering the pressure pulse and the initial rise of the current), 40 ms; time-to-peak (the time from the initial rise of the current to its peak), 199 ms; recovery time (the time it took from the peak of the current to relax back to baseline), 2300 ms; deactivation time constant, 620 ms. These results are representative of a total of 39 VSNs. Holding potential, −70 mV.

(C) Plot of the I-V relationship of a sensory current reveals the corresponding conductance change. The curve was produced in response to a voltage ramp (duration, 50 ms; slope −3.2 mV/ms) elicited at the peak of the response. A control I-V curve obtained in the absence of a sensory stimulus was digitally subtracted from the data. Data points were fitted by a polynomial function.

(D) Replacement of all extracellular cations by $NMDG^+$ eliminates the sensory current.

(E) Lowering the extracellular Ca^{2+} concentration from 1 mM (normal Ca^{2+}) to 10 μM (low Ca^{2+}) increases the peak amplitude of both the SAG- and the urine-evoked current. Note that the extent of this effect is almost identical for both types of currents. SAG concentration was 20 μM. Currents are normalized to the mean of the response obtained in normal Ca^{2+}.

(F and G) Treatment with 2-ABP (50 μM) abolishes both the SAG- and the urine-evoked current. This effect was partially reversible (data not shown).

lites (Chyb et al., 1999; Estacion et al., 2001; Hardie, 2003). Similarly, it has been suggested, based on Ca^{2+} measurements in the cell soma, that arachidonic acid or other PUFAs may play a role in VSN signal transduction (Spehr et al., 2002). To determine whether activation of the pheromone-evoked current depends on endogenously produced DAG or arachidonic acid, we used pharmacological inhibitors of enzymes participating in phospholipid and phosphatidylinositide second messenger cascades (Figures 6A and 6B). We found that an inhibitor of PLC, U-73122 (10 μM), blocks the urine-evoked sensory current, whereas an inactive structural analog, U-73343 (10 μM), had no measurable effect on this response, in accord with previous studies using action potential recordings (Inamura et al., 1997a; Holy et al., 2000). These findings provide further evidence that the pheromone-induced current recorded here is indeed responsible for the increase in stimulus-induced action potential firing. If arachidonic acid is involved in activation of this current, one would expect it to be synthesized either from phospholipids by phospholipase A_2 or from DAG by DAG lipase. However, neither isotetrandrine (10 μM, n = 3), an antagonist of phospolipase A_2, nor RHC-80267 (50 μM, n = 7), an inhibitor of DAG lipase, blocked the sensory current (Figures 6A and 6B). Furthermore, two antagonists of enzymes that metabolize arachidonic acid, the cyclooxygenase inhibitor indomethacine (50 μM, n = 3) and the lipoxygenase inhibitor nordihydroguaiaretic acid (100 or 500 μM, n = 9), did not evoke noticeable currents (data not shown). We conclude, therefore, that activation of the sensory current does not depend critically on the production of arachidonic acid or its downstream metabolites. We also tested whether phosphatidylinositol 3-kinase is involved in activation of the sensory response; however, LY-294002 (50 μM), an inhibitor of this enzyme, had no significant effect on the sensory current (Figure 6B).

The preceding results establish PLC as a key enzyme in the activation mechanism of the sensory current, consistent with our notion that an increase in the concentration of DAG initiates this current; however, they do not rule out an involvement of Ins(1,4,5)P_3, the second product of PLC activity. Although the channels formed by TRPC2 are not directly activated by Ins(1,4,5)P_3 in excised membrane patches (Figure 3), we considered the possibility that Ins(1,4,5)P_3 was somehow involved in the generation of the sensory current, as suggested by several researchers (Inamura et al., 1997b; Taniguchi et al., 2000; Gjerstad et al., 2003). To address this long-standing question, we dialyzed Ins(1,4,5)P_3 from the patch pipette directly into VSNs. For direct comparison of the resulting whole-cell currents to those evoked by pheromones or DAG, we used the same ionic conditions and voltage protocols as in the preceding experiments (Figures 4 and 5). This analysis produced three independent lines of evidence that, collectively, led us to conclude that generation of Ins(1,4,5)P_3 does not represent a primary step for activation of the pheromone conductance.

First, in no case (n = 22) did the dialysis of Ins(1,4,5)P_3 (100 μM) produce a reliable, rapidly activating membrane current (Figure 6C). In contrast, dialysis of 20 μM SAG produced an inward current that was fully active after only ≈100 ms following patch rupture (n = 4) (Figure 6C). Thus, the kinetic features of the DAG-gated channel make it well suited to account for the onset kinetics of the pheromone conductance.

Second, in a subset of VSNs (9 of 22, 41%), we observed a strongly delayed, Ins(1,4,5)P_3-dependent inward current (Figures 6D and 6E). The delay between patch rupture and initiation of this current typically ranged from 4 to 10 min. We found that this current could be mimicked by application of the Ca^{2+}-ATPase inhibitor thapsigargin (1 μM, n = 3) (Figure 6F), a procedure that induces store-dependent Ca^{2+} mobilization,

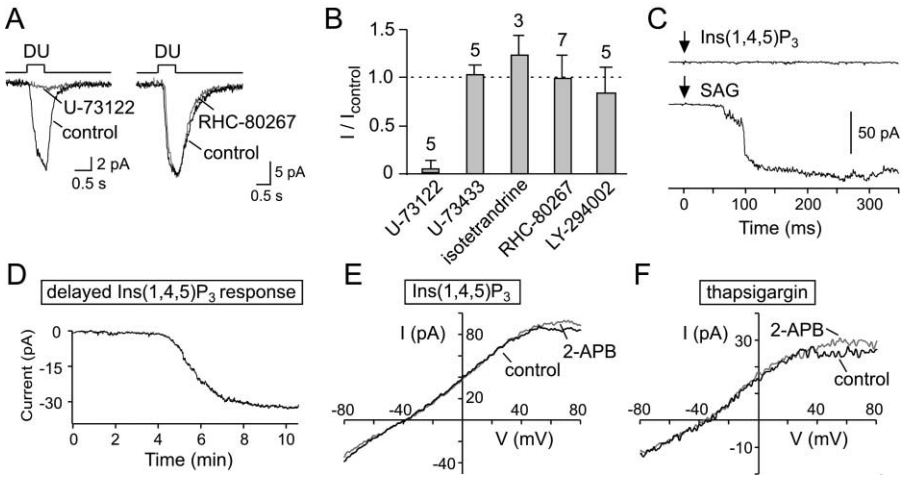

Figure 6. Evidence that the Pheromone-Evoked Conductance Depends on Endogenous DAG

(A) The pheromone-evoked current is inhibited by the PLC antagonist U73122 (10 μM) but not by an antagonist of DAG lipase, RHC-80267 (50 μM).

(B) Summary of the effects on urine-evoked currents of enzyme inhibitors of phospholipid and phosphatidylinositide signaling cascades. Each response was normalized to its own control response obtained before application of each drug as shown in (A). See text for rationale. Number of experiments are indicated above each bar. This pharmacological profile was confirmed using extracellular single-unit or field potential recordings (data not shown).

(C) VSN whole-cell currents in response to dialysis of the cells with $Ins(1,4,5)P_3$ (100 μM, upper trace) or SAG (20 μM, lower trace). Note that SAG induces a rapidly activating inward current, whereas $Ins(1,4,5)P_3$ does not. Arrows indicate rupture of the cells. Holding potential, −70 mV.

(D) Dialysis of 100 μM $Ins(1,4,5)P_3$ produces a delayed inward current in a subset of VSNs. The current typically activated after a delay of several minutes and slowly rose to a plateau over the time course of another 2–3 min. Holding potential, −70 mV.

(E) I-V relationship of the delayed $Ins(1,4,5)P_3$-induced current. Note that 2-APB (50 μM) does not inhibit this response.

(F) The effect of $Ins(1,4,5)P_3$ can be mimicked by treatment with the Ca^{2+}-ATPase inhibitor thapsigargin (1 μM).

or by direct dialysis of Ca^{2+} (500 μM) into VSNs (data not shown). We conclude, therefore, that this delayed response is not directly activated by $Ins(1,4,5)P_3$, but rather by Ca^{2+}. Because neither the TRPC2-dependent channel (Figure 1) nor the pheromone-evoked conductance (Figure 5) require Ca^{2+} for activation, $Ins(1,4,5)P_3$ is unlikely to be the primary second messenger mediating activation of the sensory current.

Third, unlike the DAG- or pheromone-induced currents, the currents evoked by $Ins(1,4,5)P_3$ or thapsigargin displayed a reversal potential at surprisingly negative voltages ranging between −30 mV and −40 mV (n = 11) (Figures 6E and 6F). The negative value of this reversal most likely reflects the combined activity of Ca^{2+}-dependent nonselective cation channels and K^+ channels (Liman, 2003; and data not shown). Furthermore, the shape of the I-V curve for both $Ins(1,4,5)P_3$ (Figure 6E) and thapsigargin (Figure 6F) was markedly different from that induced by DAG or pheromone stimulation. We also found that the responses to $Ins(1,4,5)P_3$ or thapsigargin were not blocked by 2-APB (50 μM) (Figures 6E and 6F).

Hence, unlike the DAG-gated channel, the kinetic, ionic, and pharmacological profile of the $Ins(1,4,5)P_3$-induced response fails to match that of the pheromone-evoked conductance.

A Diacylglycerol Kinase Regulates DAG Concentration in VSNs

If the pheromone-evoked conductance depends on endogenously produced DAG, an enzymatic pathway should exist in VSNs by which DAG levels are attenuated. Diacylglycerol kinase (DGK) phosphorylates DAG to produce phosphatidic acid (PA) and is, therefore, a potential terminator of DAG signaling (van Blitterswijk and Houssa, 2000; Raghu et al., 2000). To determine whether DGK exists in VSNs, we used the DGK inhibitor R59949, which appears to be specific for type I, Ca^{2+}-activated DGK isotypes (van Blitterswijk and Houssa, 2000). We found that application of R59949 (20 μM) produced a sustained activation of the TRPC2-dependent channel in voltage-clamped VSNs (n = 6) (Figures 7A–7D). This effect was dependent on the presence of Mg-ATP (1 mM) in the patch pipette solution, consistent with DGK-mediated phosphorylation (n = 5). We observed a similar effect following application of the competitive DGK inhibitor N-octanoyl sphingosine (10 μM, also known as C8-ceramide, data not shown) (Younes et al., 1992). On the basis of these results, we conclude that VSNs express an active DGK which regulates the concentration of endogenously generated DAG. These experiments suggest some basal activity of PLC because the DAG-gated channel could be activated by inhibition of a DAG-metabolizing enzyme. If so, the R59949-evoked conductance, unlike the SAG-induced conductance, should be blockable by the PLC inhibitor U-73122 (10 μM). Figures 7A and 7B demonstrate that this was indeed the case. Thus, our findings in mouse VSNs, using pharmacological blockade of DGK, resemble the constitutively active TRP channels in the *Drosophila* DGK mutant *rdgA* (Raghu et al., 2000). They are also reminiscent of the effect of phosphodiesterase inhibitors on the activity of cyclic nucleotide-gated channels in olfactory sensory neurons (Firestein et al.,

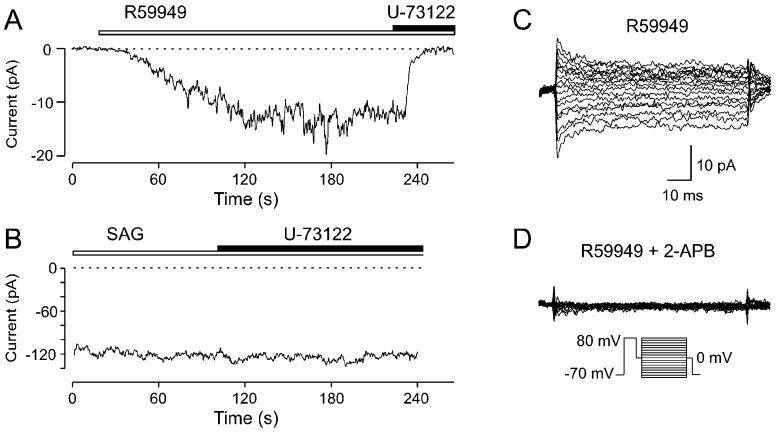

Figure 7. A Diacylglycerol Kinase Regulates DAG Concentration in VSNs

(A) Application of the type I DGK inhibitor R59949 (20 μM) produces a sustained inward current in voltage-clamped VSNs, an effect that is reversed by the PLC inhibitor U-73122 (10 μM). The current depends on the presence of MgATP (1 mM) in the patch pipette solution, consistent with DGK-mediated phosphorylation. Following the application of U-73122, there is a delay of 40 s before the current deactivates (with a time constant of 830 ms). Membrane potential, −70 mV.

(B) U-73122 (10 μM) has no effect when the current is directly activated by SAG (20 μM), indicating that the R59949-evoked conductance results from DAG build-up due to some basal activity of PLC occurring in the absence of receptor stimulation.

(C and D) R59949 (20 μM) evokes a conductance with the same properties as that induced by SAG or pheromones. The conductance has a reversal potential close to 0 mV and is inhibited by 2-APB (50 μM) (D). The presence of 1 mM Mg^{2+} in the intracellular solution in this experiment produced a slight reduction of the outward current. Currents evoked by 20 μM R59949 reached a size ranging from −8 to −43 pA (at −70 mV), which is in the same range as the pheromone-evoked current (Figure 5). Only a few picoamperes of inward current are sufficient in these cells to evoke action potential firing. Using the dose-response relationship of SAG-evoked currents in wt VSNs as a calibration (Figure 4I), we estimate that VSNs produce less than 10 μM DAG during a pheromone response.

1991). Hence, we conclude that the transduction of sensory cues in the mammalian accessory olfactory system depends primarily on channel gating by endogenously produced DAG.

Concluding Remarks

Identifying the signal transduction mechanism in pheromone-sensitive VSNs is an important step in understanding how the accessory olfactory system encodes social and reproductive information that is essential for reproductive fitness. Our experiments using excised patch clamp recordings in freshly dissociated mouse VSNs have revealed a novel DAG-activated cation channel that exists in high density in the plasma membrane of dendritic endings of these neurons. The channel can be gated effectively by the endogenous DAG analog 1-stearoyl-2-arachidonoyl-*sn*-glycerol but not by a monoacylglycerol or by Ins(1,4,5)P_3. Channel activation by DAG does not require Ca^{2+}, Mg^{2+}, or protein kinase C. Biophysical analysis demonstrates that the channel shows none of the hallmarks of capacitative Ca^{2+} release-activated Ca^{2+} channels, such as high Ca^{2+} permeability, low unitary conductance, or inward rectification (Parekh and Penner, 1997; Lewis, 1999). In addition, we demonstrate that the channel, within its native cellular environment, is not activated by treatments that induce Ca^{2+} store depletion. We conclude, therefore, that the DAG-gated channel is not primarily a store-operated channel.

A key result of the present study is the demonstration that targeted ablation of an essential component of VNO transduction, the *TRPC2* gene (Liman et al., 1999; Leypold et al., 2002; Stowers et al., 2002), causes a striking deficit in the activation of the newly identified DAG-gated channel. The residual DAG-gated conductance in *TRPC2*$^{-/-}$ VSNs differs significantly from the wt conductance in the shape of its I-V curve. On the basis of these results, we conclude that *TRPC2* encodes a principal subunit of the DAG-gated channel. This conclusion contrasts with a previous proposal suggesting that *TRPC2* encodes a store depletion-activated Ca^{2+} entry channel that may be activated through a direct interaction between an Ins(1,4,5)P_3 receptor and the TRPC2 subunit (Vannier et al., 1999; Brann et al., 2002). Regardless of whether or not such a complex is formed in intact VSNs, our results argue that this interaction would not be essential for activation of the TRPC2-dependent channel, because the channel did not open in response to Ins(1,4,5)P_3 elevation or Ca^{2+} store depletion. However, because of the existence of different splice variants of TRPC2 (Yildirim et al., 2003, and references therein), future work should address functional differences of these variants with respect to Ins(1,4,5)P_3 receptor binding.

Having identified DAG as a ligand for the TRPC2 channel, we asked whether endogenously produced DAG is responsible for activation of the pheromone-induced conductance and whether the DAG-activated channel can account for the properties of this conductance. Several lines of evidence establish that the functional profile of the pheromone-evoked current matches that of the DAG-induced current, including the relatively rapid activation kinetics, the ionic and biophysical properties, the Ca^{2+}-dependence, and the novel block by 2-APB. We also demonstrate that activation of the pheromone-evoked conductance depends critically on phospholipase C but not on phospholipase A_2 or DAG lipase, ruling out an essential role for arachidonic acid and other PUFAs in the primary transduction mechanism. As further evidence for endogenous DAG formation, we demonstrate that DAG kinase mediates an enzymatic pathway in VSNs that serves to attenuate DAG signaling; blockade of this pathway leads to intracellular build-up of DAG followed by opening of the same ion channels as those induced by exogenous DAG or pheromones. Finally, we searched extensively for Ins(1,4,5)P_3-gated cation channels that had been proposed by others to underlie VSN transduction but found no evidence for the existence of such channels.

Our findings differ from those of Spehr et al. (2002) in that we were unable to inhibit the pheromone-evoked response by the DAG lipase inhibitor RHC-80267. This difference may reflect differences in the recording methods used in these two studies, i.e., Ca^{2+} imaging at the cell soma in the case of Spehr et al. (2002) *versus* recording of the pheromone-evoked conductance in voltage-clamped VSNs in our case. Thus, it is possible that arachidonic acid or other PUFAs in VSNs may be involved in the generation of a secondary Ca^{2+} wave downstream from the primary signal transduction step, not unlike the secondary Ca^{2+} elevations observed in olfactory sensory neurons (Zufall et al., 2000). High-resolution Ca^{2+} imaging methods such as those established previously for the main olfactory epithelium (Leinders-Zufall et al., 1998) will be required to address this question. In preliminary experiments, we tested whether exogenously applied arachidonic acid evokes an inward current in VSNs, as suggested by Spehr et al. (2002). Although this was indeed the case, we found that the arachidonic acid-evoked conductance, unlike the pheromone conductance, was not inhibited by 2-ABP (50 μM) (K.U., F.Z., and T.L.-Z., unpublished data). Thus, the identity of the channels that are sensitive to arachidonic acid is currently unclear and remains to be investigated.

Collectively, our results establish the DAG-gated channel as the primary conductance pathway in a pheromone-stimulated second messenger cascade of mouse VSNs and strongly support the notion that activation of the pheromone conductance depends primarily on endogenously produced DAG. Hence, we propose a model in which ligand binding to G protein-coupled vomeronasal receptors, through stimulation of an isoform of phospholipase C (most likely PLCβ2, T.L.-Z. and F.Z., unpublished data), produces an increase in the concentration of DAG or its endogenous analogs. In turn, this second messenger signal, by a direct effect on the cation channel reported here, initiates the sensory current that underlies the depolarizing receptor potential to pheromones and other semiochemicals. Termination of DAG signaling occurs, at least in part, through the activity of a DAG kinase. This transduction mechanism is significantly different from other previously proposed models (see Introduction). It also differs from the mechanisms underlying sensory transduction in the vertebrate visual and main olfactory systems, which both employ cation channels directly gated by cyclic nucleotides (Yau and Baylor, 1989; Zufall et al., 1994; Zagotta and Siegelbaum, 1996).

The DAG-gated channel reported here not only provides a mechanism by which molecular cues are transduced into neuronal excitation, but, through its Ca^{2+} permeability, also allows extracellular Ca^{2+} to enter VSN microvilli and dendrites. We have previously shown that pheromone stimulation produces a global Ca^{2+} elevation in mouse VSNs (Leinders-Zufall et al., 2000). Interestingly, this Ca^{2+} rise is abolished by removal of extracellular Ca^{2+}, consistent with the notion that Ca^{2+} entry through the DAG-gated channel serves as the primary Ca^{2+} signal following receptor activation. What could be the function of this Ca^{2+} entry signal? Our results suggest that, as in the main olfactory epithelium (Zufall and Leinders-Zufall, 2000), stimulus-induced Ca^{2+} elevations in VSNs may serve as negative and/or positive feedback signals that are involved in regulation of the overall gain and amplification of the signal transduction machinery. In analogy to the main olfactory system (Munger et al., 2001; and references therein), one aspect of such regulation may occur at the transduction channels themselves, possibly through the recently discovered calmodulin binding site of TRPC2 (Yildirim et al., 2003). Another aspect of such Ca^{2+} feedback may involve the Ca^{2+}-activated cation (CaNS) channel reported by Liman (2003). Given our results of Figure 6, we propose that this channel may further amplify the primary sensory response. Depending on the exact location of the CaNs channel, i.e., whether or not it is present in the VSN microvilli, this amplification may occur via Ca^{2+} that enters the cell through the DAG-gated channel or via store-operated Ca^{2+} mobilization mediated by Ins(1,4,5)P_3 or both. Future experiments should address these questions.

Finally, it is important to note that our findings may have implications beyond the sense of smell in that they provide a general mechanism by which PLC signaling can produce neuronal excitation and Ca^{2+} entry, independently of protein kinase C, Ins(1,4,5)P_3, and Ca^{2+} stores. Based on the use of heterologous expression systems, several recent studies have proposed that the TRP channel subunits hTRPC3, hTRPC6, and mTRPC7 may function as DAG-gated channels (Hofmann et al., 1999; Okada et al., 1999; Venkatachalam et al., 2001). However, there has been some controversy regarding the physiological significance of this activation mechanism (Kiselyov and Muallem, 1999). Our results provide definitive evidence for a specific function of native DAG-gated cation channels in the mammalian nervous system: pheromone sensing. It should be interesting to determine whether this signal transduction theme is employed more generally in the brain.

Experimental Procedures

Animals

All experiments were performed on 30- to 90-day-old CD-1 mice, except for those presented in Figure 4, which used *TRPC2*$^{+/-}$ breeding pairs of mixed 129SvEv $\times$ C57BL/6J background to produce *TRPC2*$^{-/-}$ animals or wild-type (wt) littermate controls of the same age. Generation of these mice has been described (Leypold et al., 2002). No obvious differences exist in SAG-induced whole-cell currents between wt CD-1 or 129SvEv $\times$ C57BL6/J mice.

Tissue Preparation

Mice were decapitated, following anesthesia, and the vomeromasal organ was removed (Leinders-Zufall et al., 2000). For the preparation of singly dissociated VSNs, the tissue was minced and digested at 37°C for 15 min in 0.19 mg/ml papain (Sigma) and 1 U/ml DNase (Promega) in a Ca^{2+}-buffered, oxygenated (95% O_2/5% CO_2) extracellular solution containing 120 mM NaCl, 25 mM $NaHCO_3$, 5 mM KCl, 5 mM BES, 1 mM $MgSO_4$, 4.8 mM $CaCl_2$, 5 mM EGTA, 10 mM NaOH, 10 mM glucose. The tissue was then washed in standard extracellular solution (ES1: 120 mM NaCl, 25 mM $NaHCO_3$, 5 mM KCl, 5 mM BES, 1 mM $MgSO_4$, 1 mM $CaCl_2$, 10 mM mM glucose), centrifuged for 10 min at 600 rpm, and the pellet resuspended using ES1. Gentle trituration through a fire-polished Pasteur pipette resulted in the release of single cells. Cells were stored at 4°C and plated immediately before use on glass coverslips coated with 0.01% poly-L-lysine and 0.1% laminin. For the experiments of Figures 5, 6A, and 6B, VNO tissue slices were prepared as described, and infrared videomicroscopy was used to optically identify single VSNs (Leinders-Zufall et al., 2000).

Electrophysiological Recording and Data Analyses

Inside-out patch recordings were made as described (Zufall and Hatt, 1991; Zufall et al., 1991). Isolated membrane patches excised from the dendritic tip of VSNs were transferred to a separate chamber that permitted exchange of the solution surrounding the membrane patch without contamination of the cell population (Warner Intruments). Standard pipette solution in inside-out experiments was 140 mM NaCl, 10 mM Na-HEPES, 1 mM EGTA (pH 7.3) (HCl); adjusted to 290 mOsm (glucose). The bath solutions contained *Na^+-based*, 140 mM NaCl, 10 mM Na-HEPES, 1 mM EGTA; *Cs^+-based*, 140 mM CsCl, 4 mM CsOH, 10 mM HEPES, 1 mM EGTA; *$NMDG^+$-based*, 140 mM NMDG, 135 mM HCl, 10 mM HEPES, 1 mM EGTA; *Ca^{2+}-based*, 90 mM $CaCl_2$, 10 mM HEPES (pH 7.1), 290 mOsm (glucose). Single-channel event and time analyses were performed using TAC 4.1.4 software (Bruxton). Relative permeability ratios were calculated using the Goldman-Hodgkin-Katz equations for bi-ionic conditions (Lewis, 1979). Whole-cell recordings were performed using the following pipette solution 140 mM CsCl, 2 mM CsOH, 1 mM EGTA, 10 mM HEPES (pH 7.1) (CsOH) and 290 mOsm (glucose). For experiments that used dilute urine as a stimulus, this solution was supplemented with 1 mM Na-ATP and 0.5 mM Na-GTP and Cs^+ was replaced by K^+ in some experiments. Standard ES1 without added $MgSO_4$ was used in the bath. An EPC-9 patch-clamp amplifier was used for all current- and voltage-clamp recordings, command potential sequences, data acquisition, and online analyses. If not otherwise stated, data are expressed as means ± SD.

Chemical Stimulation

Stock solutions of the DAG analogs SAG, DOG, OAG (all from Calbiochem), and OG (Alexis) were prepared in DMSO and aliquots stored at −20°C. Final dilutions using bath medium were made immediately before use, briefly sonicated, and directly added to the recording chamber. Final DMSO concentrations (≤0.1%) used were also tested alone in controls and had no effect. In one type of experiment (Figure 6C), SAG was dialyzed directly from the patch pipette into VSNs. Other pharmacological agents such as U-73122 (BioMol), U-73343 (BioMol), 2-APB (BioMol), RHC-80267 (BioMol), LY-294002 (BioMol), isotetrandrine (BioMol), indomethacine (Calbiochem), NDGA (Calbiochem), calphostin C (BioMol), staurosporine (BioMol), R59949 (Calbiochem), N-octanoyl sphingosine (Calbiochem), and thapsigargin (Alexis) were applied through the bath. Thapsigargin was prepared as described (Zufall et al., 2000). Fresh urine, a rich source of natural pheromones, was collected daily from male and female mice, diluted 100-fold, and focally ejected onto VSN microvilli as described (Leinders-Zufall et al., 2000; Leypold et al., 2002). Artificial urine (Leypold et al., 2002) at a dilution of 1/100 gave no measurable responses in single VSNs.

Acknowledgments

This study was supported by grants from INRA, NATO, and the Philippe Foundation to P.L. and the NIH/NIDCD to T.L.-Z. and F.Z. We thank Xia-Hong Li for excellent technical assistance; Richard Axel for providing TRPC2 knockout mice; Faith Scipio and Frank Margolis for help with genotyping; Steven Munger and David Litwack for comments on an earlier version of this manuscript; and Chris Miller for a stimulating discussion.

Received: July 31, 2003
Revised: September 15, 2003
Accepted: September 24, 2003
Published: October 29, 2003

References

Bootman, M.D., Collins, T.J., Mackenzie, L., Roderick, H.L., Berridge, M.J., and Peppiatt, C.M. (2002). 2-Aminoethoxydiphenyl borate (2-APB) is a reliable blocker of store-operated Ca^{2+} entry but an inconsistent inhibitor of $InsP_3$-induced Ca^{2+} release. FASEB J. *16*, 1145–1150.

Boschat, C., Pelofi, C., Randin, O., Roppolo, D., Luscher, C., Broillet, M.C., and Rodriguez, I. (2002). Pheromone detection mediated by a V1r vomeronasal receptor. Nat. Neurosci. *5*, 1261–1262.

Brann, J.H., Dennis, J.C., Morrison, E.E., and Fadool, D.A. (2002). Type-specific inositol 1,4,5-trisphosphate receptor localization in the vomeronasal organ and its interaction with a transient receptor potential channel, TRPC2. J. Neurochem. *83*, 1452–1460.

Chyb, S., Raghu, P., and Hardie, R.C. (1999). Polyunsaturated fatty acids activate the *Drosophila* light-sensitive channels TRP and TRPL. Nature *397*, 255–259.

Cinelli, A.R., Wang, D., Chen, P., Liu, W., and Halpern, M. (2002). Calcium transients in the garter snake vomeronasal organ. J. Neurophysiol. *87*, 1449–1472.

Clapham, D.E., Runnels, L.W., and Strübing, C. (2001). The TRP ion channel family. Nat. Rev. Neurosci. *2*, 387–396.

Del Punta, K., Leinders-Zufall, T., Rodriguez, I., Jukam, D., Wysocki, C.J., Ogawa, S., Zufall, F., and Mombaerts, P. (2002). Deficient pheromone responses in mice lacking a cluster of vomeronasal receptor genes. Nature *419*, 70–74.

Dulac, C., and Torello, A.T. (2003). Molecular detection of pheromone signals in mammals: from genes to behaviour. Nat. Rev. Neurosci. *4*, 551–562.

Estacion, M., Sinkins, W.G., and Schilling, W.P. (2001). Regulation of *Drosophila* transient receptor potential-like (TrpL) channels by phospholipase C-dependent mechanisms. J. Physiol. *530*, 1–19.

Firestein, S., Zufall, F., and Shepherd, G.M. (1991). Single odor-sensitive channels in olfactory receptor neurons are also gated by cyclic nucleotides. J. Neurosci. *11*, 3565–3572.

Gjerstad, J., Valen, E.C., Trotier, D., and Døving, K. (2003). Photolysis of caged inositol 1,4,5-trisphosphate induces action potentials in frog vomeronasal microvillar receptor neurones. Neuroscience *119*, 193–200.

Goñi, F.M., and Alonso, A. (1999). Structure and functional properties of diacylglycerols in membranes. Prog. Lipid Res. *38*, 1–48.

Hardie, R.C. (2003). Regulation of TRP channels via lipid second messengers. Annu. Rev. Physiol. *65*, 735–759.

Hofmann, T., Obukhov, A.G., Schaefer, M., Harteneck, C., Gudermann, T., and Schultz, G. (1999). Direct activation of human TRPC6 and TRPC3 channels by diacylglycerol. Nature *397*, 259–263.

Hofmann, T., Schaefer, M., Schultz, G., and Gudermann, T. (2000). Cloning, expression and subcellular localization of two novel splice variants of mouse transient receptor potential channel 2. Biochem. J. *351*, 115–122.

Hofmann, T., Schaefer, M., Schultz, G., and Gudermann, T. (2002). Subunit composition of mammalian transient receptor potential channels in living cells. Proc. Natl. Acad. Sci. USA *99*, 7461–7466.

Holy, T.E., Dulac, C., and Meister, M. (2000). Responses of vomeronasal neurons to natural stimuli. Science *289*, 1569–1572.

Inamura, K., and Kashiwayanagi, M. (2000). Inward current responses to urinary substances in rat vomeronasal sensory neurons. Eur. J. Neurosci. *12*, 3529–3536.

Inamura, K., Kashiwayanagi, M., and Kurihara, K. (1997a). Blockage of urinary responses by inhibitors for IP_3-mediated pathway in rat vomeronasal sensory neurons. Neurosci. Lett. *233*, 129–132.

Inamura, K., Kashiwayanagi, M., and Kurihara, K. (1997b). Inositol-1,4,5-triphosphate induces responses in receptor neurons in rat vomeronasal sensory slices. Chem. Senses *22*, 93–103.

Inamura, K., Matsumotu, Y., Kashiwayanagi, M., and Kurihara, K. (1999). Laminar distribution of pheromone-receptive neurons in rat vomeronasal epithelium. J. Physiol. *517*, 731–739.

Johnston, R.E. (1998). Pheromones, the vomeronasal system, and communication: from hormonal responses to individual recognition. Ann. N Y Acad. Sci. *855*, 333–348.

Keverne, E.B. (2002). Mammalian pheromones: from genes to behavior. Curr. Biol. *12*, R807–R809.

Kiselyov, K., and Muallem, S. (1999). Fatty acids, diacylglycerol, $Ins(1,4,5)P_3$ receptors and Ca^{2+} influx. Trends Neurosci. *22*, 334–337.

Krieger, J., Schmitt, A., Löbel, D., Gudermann, T., Schultz, G., Breer, H., and Boekhoff, I. (1999). Selective activation of G protein subtypes in the vomeronasal organ upon stimulation with urine-derived compounds. J. Biol. Chem. *274*, 4655–4662.

Kroner, C., Breer, H., Singer, A.G., and O'Connell, R.J. (1996). Pheromone-induced second messenger signaling in the hamster vomeronasal organ. Neuroreport *7*, 2989–2992.

Leinders-Zufall, T., Greer, C.A., Shepherd, G.M., and Zufall, F. (1998). Imaging odor-induced calcium transients in single olfactory cilia: specificity of activation and role in transduction. J. Neurosci. *18*, 5630–5639.

Leinders-Zufall, T., Lane, A.P., Puche, A.C., Ma, W., Novotny, M., Shipley, M.T., and Zufall, F. (2000). Ultrasensitive pheromone detection by mammalian vomeronasal neurons. Nature *405*, 792–796.

Lewis, C.A. (1979). Ion-concentration dependence of the reversal potential and the single channel conductance of ion channels at the frog neuromuscular junction. J. Physiol. *286*, 417–445.

Lewis, R.S. (1999). Store-operated calcium channels. Adv. Second Messenger Phosphoprotein Res. *33*, 279–307.

Leypold, B.G., Yu, C.R., Leinders-Zufall, T., Kim, M.M., Zufall, F., and Axel, R. (2002). Altered sexual and social behaviors in trp2 mutant mice. Proc. Natl. Acad. Sci. USA *99*, 6376–6381.

Liman, E.R. (2003). Regulation by voltage and adenine nucleotides of a Ca^{2+}-activated cation channel from hamster vomeronasal sensory neurons. J. Physiol. *548*, 777–787.

Liman, E.R., and Innan, H. (2003). Relaxed selective pressure on an essential component of pheromone transduction in primate evolution. Proc. Natl. Acad. Sci. USA *100*, 3328–3332.

Liman, E.R., Corey, D.P., and Dulac, C. (1999). TRP2: A candidate transduction channel for mammalian pheromone sensory signaling. Proc. Natl. Acad. Sci. USA *96*, 5791–5796.

Loconto, J., Papes, F., Chang, E., Stowers, L., Jones, E.P., Takada, T., Kumanovics, A., Fischer Lindahl, K., and Dulac, C. (2003). Functional expression of murine V2R pheromone receptors involves selective association with the M10 and M1 families of MHC class Ib molecules. Cell *112*, 607–618.

Luo, Y., Lu, S., Chen, P., Wang, D., and Halpern, M. (1994). Identification of chemoattractant receptors and G-proteins in the vomeronasal system of garter snakes. J. Biol. Chem. *269*, 16867–16877.

Luo, M., Fee, M.S., and Katz, L.C. (2003). Encoding pheromonal signals in the accessory olfactory bulb of behaving mice. Science *299*, 1196–1201.

Menco, B.P., Carr, V.M., Ezeh, P.I., Liman, E.R., and Yankova, M.P. (2001). Ultrastructural localization of G-proteins and the channel protein TRP2 to microvilli of rat vomeronasal receptor cells. J. Comp. Neurol. *438*, 468–489.

Montell, C., Birnbaumer, L., and Flockerzi, V. (2002). The TRP channels, a remarkably functional family. Cell *108*, 595–598.

Munger, S.D., Lane, A.P., Zhong, H., Leinders-Zufall, T., Yau, K.-W., Zufall, F., and Reed, R.R. (2001). Central role of the CNGA4 channel subunit in Ca^{2+}-calmodulin-dependent odor adaptation. Science *294*, 2172–2175.

Norlin, E.M., Gussing, F., and Berghard, A. (2003). Vomeronasal phenotype and behavioral alterations in Gαi2 mutant mice. Curr. Biol. *13*, 1214–1219.

Okada, T., Inoue, R., Yamazaki, K., Maeda, A., Kurosaki, T., Yamakuni, T., Tanaka, I., Shimizu, S., Ikenaka, K., Imoto, K., and Mori, Y. (1999). Molecular and functional characterization of a novel mouse transient receptor potential protein homologue TRP7. J. Biol. Chem. *274*, 27359–27370.

Parekh, A.B., and Penner, R. (1997). Store depletion and calcium influx. Physiol. Rev. *77*, 901–930.

Raghu, P., Usher, K., Jonas, S., Chyb, S., Polyanovsky, A., and Hardie, R.C. (2000). Constitutive activity of the light-sensitive channels TRP and TRPL in the *Drosophila* diacylglycerol kinase mutant, *rdgA*. Neuron *26*, 169–179.

Sam, M., Vora, S., Malnic, B., Ma, W., Novotny, M.V., and Buck, L.B. (2001). Odorants may arouse instinctive behaviours. Nature *412*, 142.

Sasaki, K., Okamoto, K., Inamura, K., Tokumitsu, Y., and Kashiwayanagi, M. (1999). Inositol-1,4,5-triphosphate accumulation induced by urinary pheromones in female rat vomeronasal epithelium. Brain Res. *823*, 161–168.

Spehr, M., Hatt, H., and Wetzel, C.H. (2002). Arachidonic acid plays a role in rat vomeronasal signal transduction. J. Neurosci. *22*, 8429–8437.

Stowers, L., Holy, T.E., Meister, M., Dulac, C., and Koentges, G. (2002). Loss of sex discrimination and male-male aggression in mice deficient for TRP2. Science *295*, 1493–1500.

Taniguchi, M., Kashiwayanagi, M., and Kurihara, K. (1995). Intracellular injection of inositol 1,4,5-trisphosphate increases a conductance in membranes of turtle vomeronasal receptor neurons in the slice preparation. Neurosci. Lett. *188*, 5–8.

Taniguchi, M., Wang, D., and Halpern, M. (2000). Chemosensitive conductance and inositol 1,4,5-triphosphate-induced conductance in snake vomeronasal receptor neurons. Chem. Senses *25*, 67–76.

Trinh, K., and Storm, D.R. (2003). Vomeronasal organ detects odorants in absence of signaling through main olfactory epithelium. Nat. Neurosci. *6*, 519–525.

Trotier, D., Døving, K.B., Ore, K., and Shalchian-Tabrizi, C. (1998). Scanning electron microscopy and gramicidin patch clamp recordings of microvillous receptor neurons dissociated from the rat vomeronasal organ. Chem. Senses *23*, 49–57.

Vannier, B., Peyton, M., Boulay, G., Brown, D., Qin, N., Jiang, M., Zhu, X., and Birnbaumer, L. (1999). Mouse trp2, the homologue of the human trpc2 pseudogene, encodes mTrp2, a store depletion-activated capacitative Ca^{2+} entry channel. Proc. Natl. Acad. Sci. USA *96*, 2060–2064.

van Blitterswijk, W.J., and Houssa, B. (2000). Properties and functions of diacylglycerol kinases. Cell. Signal. *12*, 595–605.

Venkatachalam, K., Ma, H.T., Ford, D.L., and Gill, D.L. (2001). Expression of functional receptor-coupled TRPC3 channels in DT40 triple receptor $InsP_3$ knockout cells. J. Biol. Chem. *276*, 33980–33985.

Wekesa, K.S., and Anholt, R.R.H. (1997). Pheromone regulated production of inositol-(1,4,5)-triphosphate in the mammalian vomeronasal organ. Endocrinology *138*, 3497–3504.

Yau, K.W., and Baylor, D.A. (1989). Cyclic GMP-activated conductance of retinal photoreceptor cells. Annu. Rev. Neurosci. *12*, 289–327.

Yildirim, E., Dietrich, A., and Birnbaumer, L. (2003). The mouse C-type transient receptor potential 2 (TRPC2) channel: alternative splicing and calmodulin binding to its N terminus. Proc. Natl. Acad. Sci. USA *100*, 2220–2225.

Younes, A., Kahn, D.W., Besterman, J.M., Bittman, R., Byun, H.S., and Kolesnick, R.N. (1992). Ceramide is a competitive inhibitor of diacylglycerol kinase *in vitro* and in intact human leukemia (HL-60) cells. J. Biol. Chem. *267*, 842–847.

Zagotta, W.N., and Siegelbaum, S.A. (1996). Structure and function of cyclic nucleotide-gated channels. Annu. Rev. Neurosci. *19*, 235–263.

Zhang, J., and Webb, D.M. (2003). Evolutionary deterioration of the vomeronasal pheromone transduction pathway in catarrhine primates. Proc. Natl. Acad. Sci. USA *100*, 8337–8341.

Zufall, F., and Hatt, H. (1991). Dual activation of a sex pheromone dependent ion channel from insect olfactory dendrites by protein kinase C activators and cyclic GMP. Proc. Natl. Acad. Sci. USA *88*, 8520–8524.

Zufall, F., and Leinders-Zufall, T. (2000). The cellular and molecular basis of odor adaptation. Chem. Senses *25*, 473–481.

Zufall, F., Firestein, S., and Shepherd, G.M. (1991). Analysis of single cyclic nucleotide gated channels from olfactory receptor cell dendrites. J. Neurosci. *11*, 3573–3580.

Zufall, F., Firestein, S., and Shepherd, G.M. (1994). Cyclic nucleotide-gated ion channels and sensory transduction in olfactory receptor neurons. Annu. Rev. Biophys. Biomol. Struct. *23*, 577–607.

Zufall, F., Leinders-Zufall, T., and Greer, C.A. (2000). Amplification of odor-induced Ca^{2+} transients by store-operated Ca^{2+} release and its role in olfactory signal transduction. J. Neurophysiol. *83*, 501–512.